nature communications

Article

https://doi.org/10.1038/s41467-025-63183-x

Modeling of T cell-mediated autoimmune pituitary disease using human induced pluripotent stem cell-originated organoid

Received: 30 October 2023

Accepted: 13 August 2025

Published online: 25 August 2025

Check for updates

Keitaro Kanie[1,9], Takeshi Ito[2,9], Genzo Iguchi[3], Ryusaku Matsumoto[4], Keiko Muguruma[5,6], Shin Urai[1], Shuichi Kitayama[2], Hironori Bando[7], Masaaki Yamamoto[7], Hidenori Fukuoka[7], Wataru Ogawa[1], Shin Kaneko[2] & Yutaka Takahashi[7,8]

Anti-pituitary-specific transcription factor (PIT)−1 hypophysitis is an autoimmune disease characterized by hormone secretion impairment from PIT-1-expressing pituitary cells, accompanied by malignancies with ectopic PIT-1 expression. Cytotoxic T cells (CTL) targeting PIT-1-positive cells have been implicated in disease development, yet direct evidence is lacking. As human leukocyte antigen (HLA)-matching is required for modeling T cell-mediated autoimmune diseases, we employ induced pluripotent stem cells (iPSC) to generate pituitary organoids harboring the patients' HLA haplotype and coculture the organoids with PIT-1-reactive CTLs isolated from the patients' peripheral blood mononuclear cells. The coculture demonstrates specific CTL-mediated cytotoxicity against PIT-1-positive cells exclusively in autologous conditions, with this cytotoxicity inhibited by immunosuppressive agents such as dexamethasone and cyclosporin A. Multiple combinations of epitopes, CTLs, and HLA molecules are responsible for pathogenesis. These data demonstrate CTL-mediated autoimmunity in anti-PIT-1 hypophysitis and highlight the potential application of this strategy for other T cell-mediated autoimmune diseases.

Autoimmune pituitary disease, in which the pituitary gland is injured by autoimmune mechanisms resulting in hypopituitarism or diabetes insipidus, comprises such as lymphocytic hypophysitis, IgG4-related hypophysitis, anti-pituitary-specific transcription factor (PIT)−1 hypophysitis (also known as anti-PIT-1 antibody syndrome), isolated adrenocorticotropic hormone (ACTH) deficiency, and the recently reported immune checkpoint inhibitor-related hypophysitis[1–3]. Among them, anti-PIT-1 hypophysitis is characterized by an acquired deficiency of growth hormone (GH), thyroid-stimulating hormone (TSH), and prolactin (PRL) caused by autoimmunity against PIT-1, which plays an essential role in the development and maintenance of GH-, TSH-, and PRL-producing cells[4].

In addition to the lineage-specific impairment of PIT-1-positive cells, anti-PIT-1 hypophysitis is associated with malignancies that

[1]Division of Diabetes and Endocrinology, Department of Internal Medicine, Kobe University Graduate School of Medicine, Kobe, Hyogo, Japan. [2]Shin Kaneko Laboratory, Department of Cell Growth and Differentiation, Center for iPS Cell Research and Application (CiRA), Kyoto University, Kyoto, Kyoto, Japan. [3]Medical Center for Student Health, Kobe University, Kobe, Hyogo, Japan. [4]Takuya Yamamoto Research Laboratory, Department of Cell Growth and Differentiation, CiRA, Kyoto University, Kyoto, Kyoto, Japan. [5]Department of iPS Cell Applied Medicine, Kansai Medical University, Hirakata, Osaka, Japan. [6]RIKEN Center for Biosystems Dynamics Research, Kobe, Hyogo, Japan. [7]Department of Diabetes and Endocrinology, Kobe University Hospital, Kobe, Hyogo, Japan. [8]Department of Diabetes and Endocrinology, Nara Medical University, Kashihara, Nara, Japan. [9]These authors contributed equally: Keitaro Kanie, Takeshi Ito. e-mail: takahash@naramed-u.ac.jp

ectopically express PIT-1. The ectopic expression disrupts immune tolerance toward PIT-1, leading to exclusive cell impairment in the PIT-1-positive lineage. Although immune tolerance breakdown is critical for anti-PIT-1 hypophysitis induction, the mechanism by which this specific cell impairment is induced remains unclear. Autoantibodies against PIT-1 are detected in most patients with this hypophysitis and are considered a specific biomarker for the disease. Although the detection of autoantibodies is included in its diagnostic criteria along with the acquired hormone deficiency[1], its etiological involvement is less likely[4]. However, T cell-mediated immunity has been suggested as a possible etiology based on pathological analyses and the presence of circulating PIT-1-reactive CTLs in patients[5]. The PIT-1 epitope has also been reported to be presented on HLA-molecules[6]. As T cells require epitope presentation on HLA-molecules for antigen recognition, this finding further supports the hypothesis that PIT-1 hypophysitis is induced via T cell-mediated immunity.

To recapitulate autoimmune hypophysitis, several animal models have been reported[7–10]. Although animal models are informative, matching immunological conditions, especially HLA-haplotypes, are difficult in nonhuman models. The use of induced pluripotent stem cells (iPSCs) can be a good solution for overcoming this hurdle. iPSCs can be derived from autologous specimens and differentiated into cells and organs of interest while retaining the original genetic background. This technology has been applied to establish disease models, especially of genetic disorders[11,12]. However, few models for autoimmune diseases have been developed yet. A recent study developed a model for type 1 diabetes mellitus, a T cell-mediated autoimmune disease, by coculturing iPSC-derived pancreatic beta cells and peripheral blood mononuclear cells (PBMCs)[13]. Although T cells were activated, no cytotoxicity on beta cells was observed; additionally, the responsible T cells have not yet been identified. Although the use of iPSC-derived tissues is advantageous in matching HLA antigens with patients, isolating the responsible T cells is critical for clarifying the pathophysiological mechanism in T cell-mediated autoimmune diseases[14].

Herein, we aim to establish a disease model for anti-PIT-1 hypophysitis by isolating PIT-1 specific CTLs and regenerating iPSC-derived pituitary tissue from patients. Through disease modeling, we also demonstrate the specific T cell receptor (TCR) and combinations of epitope and HLA molecules involved in this disease. The recapitulated pathological condition enables to test potential drugs for treatment. This approach not only uncovers the pathophysiology of anti-PIT-1 hypophysitis but also proposes a disease modeling strategy for T cell-mediated autoimmune diseases.

Results

Reactive CTLs and TCR isolation from patients with anti-PIT-1 hypophysitis

Both circulating PIT-1-reactive CTLs and infiltrating CD8-positive cells in the pituitary have been observed in anti-PIT-1 hypophysitis[5], suggesting the pivotal role of CTLs in disease pathogenesis. Therefore, we attempted to isolate antigen-specific CTLs from PBMCs of patients with anti-PIT-1 hypophysitis (Cases 1 and 2, Supplementary Table 1)[4,15]. Initially, we stimulated PBMCs with full-length PIT-1, but no cells proliferated in response. Subsequently, we designed 95 overlapping peptides (OPs) of 10 residues that cover full-length PIT-1 (Fig. 1a). As removal of regulatory T cells results in higher efficiency in obtaining antigen-specific activated CTLs[16], we selectively depleted the $CD4^+CD25^+$ population from PBMCs before peptide stimulation (Supplementary Fig. 1a, b). We used peptide pools (PP) containing 10 OPs each for the initial selection. As indicated by our in silico analysis for HLA-A24, PP21-30 was considered the best candidate for activating CTLs because high prediction scores from the three algorithms clustered in this region (Supplementary Fig. 1c). Screening experiments using PPs supported the in silico prediction (Supplementary Fig. 1d, e). We repeatedly stimulated PBMCs with PP21-30 to derive reactive CTLs (Fig. 1b). After repetitive stimulations with PP21-30, we found that a small fraction of CTLs was activated, as demonstrated by the presence of 4-1BB-positive cells. Moreover, subtype analysis of TCRs showed that the PP21-30 reactive CTLs had Vβ7.1 (Fig. 1c and Supplementary Fig. 2a). After the selective expansion of $V\beta7.1^+$ CTLs, we confirmed the specific activation by PP21-30 (Supplementary Fig. 2b–d). Next, we analyzed the effect of individual OPs on $V\beta7.1^+$ CTLs, revealing that OP30 specifically activated $V\beta7.1^+$ CTLs (Fig. 1d and Supplementary Fig. 2e). We also analyzed the rearrangements of the TCR genes (Fig. 1e). We detected two pairs of TCRA in the repertoire analysis of $V\beta7.1^+$ CTLs and evaluated their reactivity against OP30 by preparing TCR-expressing vectors (Supplementary Fig. 2f, i). Forced expression of TCRs on autologous peripheral blood derived-CTLs (PB-CTLs) showed that only the TRAV16/TRBV4-1 combination activated PB-CTLs in the presence of OP30 (Fig. 1f).

To confirm the reproducibility of this method for isolating reactive CTLs, we repeated the process by using different lots of PBMCs from Case 1. Accordingly, we isolated PP21-30 reactive CTLs with the same $V\beta7.1^+$ repertoire (Supplementary Fig. 3). In addition, we isolated reactive CTLs from another patient, Case 2, in the same manner (Supplementary Fig. 4). The reactive CTLs from Case 2 showed $V\beta8^+$ expression and were activated by OP21, representing a different TCR subtype and epitope pair from Case 1 (Supplementary Fig. 4b–d). These results collectively supported the reproducibility of our method for isolating reactive CTLs.

Generating functional PIT-1-expressing pituitary cells from patient-derived iPSCs

To prepare the target pituitary tissue, we used iPSCs from two patients, Case 1 and Case 2, and two control individuals (Supplementary Table 1, 2). iPSCs from Case 2 were established in the present study (Supplementary Fig. 5), whereas the rest had been reported previously[17–19]. We induced their differentiation into anterior pituitary and hypothalamic cells, as previously described[6,20,21] (Fig. 2a). We observed that control- and patient-derived iPSCs differentiated into LHX3-positive pituitary progenitor cells on day 39 and subsequently into PIT-1-positive cells on day 100 (Fig. 2b). We also generated PIT-1-GFP reporter iPSCs using the CRISPR/Cas9 system to easily track PIT-1-positive cells (Fig. 2c). We induced the differentiation of these iPSCs into pituitary cells and detected GFP expression in a region that was compatible with the oral ectoderm, which is a progenitor of the anterior pituitary gland (Fig. 2d). Immunostaining analysis demonstrated clear colocalization of PIT-1 and GFP (Fig. 2e). Furthermore, we confirmed the expression of *GH1* and *POU1F1* in pituitary organoids (Supplementary Fig. 6) and their GH-producing ability; >58% of PIT-1-positive cells were GH-positive irrespective of donors (Fig. 2f, g). GH secretion was enhanced in response to growth hormone-releasing hormone (GHRH) stimulation (Fig. 2h). These results were comparable regardless of cohorts and GFP knock-in profiles, demonstrating consistent pituitary differentiation from iPSCs.

Cytotoxicity on iPSC-derived pituitary cells mediated by autologous reactive CTLs

The HLA-epitope complex is required for a robust immune response by CTLs. Our previous study showed that the PIT-1 epitope is presented by HLA-class I via the antigen-presentation pathway in human iPSC-derived anterior pituitary cells[6]. Therefore, to establish a disease model, we cocultured patient-derived CTLs with their corresponding iPSC-derived pituitary organoids (Fig. 3a). Coculturing resulted in exclusive activation of reactive CTLs only under autologous but not under allogeneic conditions (Fig. 3b and Supplementary Fig. 7a, b). In addition, the expression of interferon-γ (*IFNG*), granzyme-B (*GZMB*), and perforin-1 (*PRF1*), which are markers of activated or cytotoxic T

https://doi.org/10.1038/s41467-025-63183-x

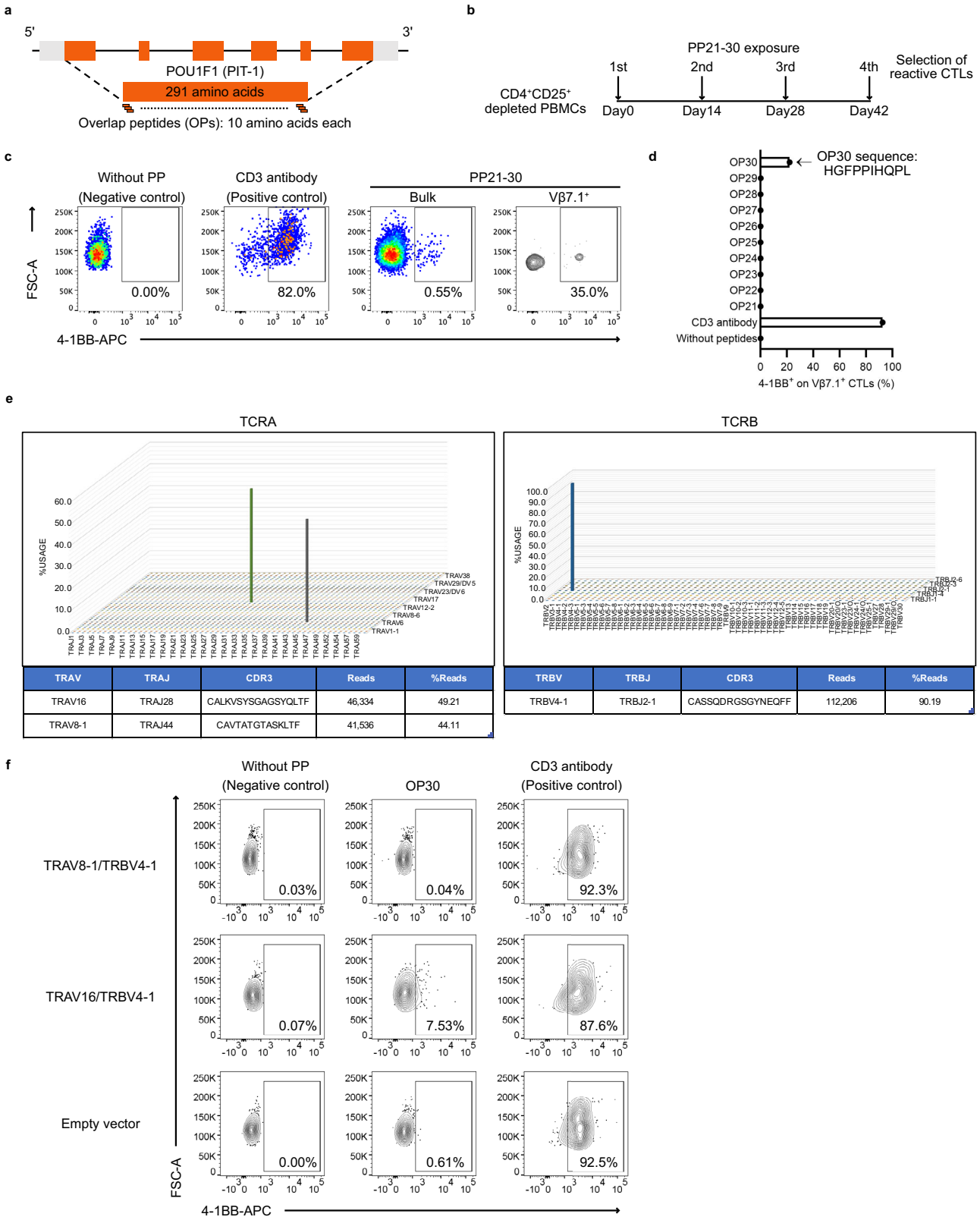

TRAV	TRAJ	CDR3	Reads	%Reads
TRAV16	TRAJ28	CALKVSYSGAGSYQLTF	46,334	49.21
TRAV8-1	TRAJ44	CAVTATGTASKLTF	41,536	44.11

TRBV	TRBJ	CDR3	Reads	%Reads
TRBV4-1	TRBJ2-1	CASSQDRGSGYNEQFF	112,206	90.19

cells, was specifically upregulated only under autologous conditions (Fig. 3c). Furthermore, we observed significant infiltration of CTLs only under autologous conditions (Fig. 3d, e and Supplementary Fig. 7c). We also observed double-positive cells for cleaved caspase-3 (CC3; a marker of apoptosis) and PIT-1 only under autologous conditions (Fig. 3f, g and Supplementary Fig. 7d). Time-lapse imaging showed that reactive CTLs from Case 1 accumulated and attacked autologous PIT-1-positive cells; after 4 h, PIT-1-positive cells were fragmented (Fig. 3h and Supplementary Movie 1).

Next, we evaluated whether antibody-dependent cellular cytotoxicity (ADCC) was involved in disease etiology. We found that in the presence of patient serum, none of the coculture conditions, including PBMCs and iPSC-derived pituitary cells of Case 1, resulted in an increase in the number of PIT-1-positive dead cells or upregulation of

Fig. 1 | Cloning of specific cytotoxic T lymphocytes (CTLs) from a patient with anti-PIT-1 hypophysitis (Case 1). a Design of overlapping peptides (OPs) for covering PIT-1. The amino acid sequence translated from the open reading frame of PIT-1 was used to design OPs. **b** Schematic of peptide pool (PP) exposure and isolation of reactive CTLs from peripheral blood mononuclear cells (PBMCs). $CD4^+CD25^+$ depleted PBMCs were prepared on day 0. PP21-30 was exposed to the $CD4^+CD25^+$ depleted PBMCs every 14 days. After four repeated exposures, the reactivity of CTLs was confirmed based on 4-1BB expression upon re-exposure to PP21-30. **c** Isolation of PP21-30 reactive CTLs on the basis of the Vβ-subtype. The 4-1BB expression was evaluated 24 h after PP21-30 exposure. Anti-CD3 antibody was used as positive control. All data were gated on live cells. Gating on $V\beta7.1^+$ was added only for the rightmost panel. **d** Determination of reactive OPs from PP21-30. The $4\text{-}1BB^+$ proportion on $V\beta7.1^+$ CTLs was evaluated 24 h after each OP exposure, and the ratio of $4\text{-}1BB^+$ cells on $V\beta7.1^+$ CTLs is shown; the original flow cytometry panels appear in Supplementary Fig. 1e. OP30 is indicated with an arrow, and its amino acid sequence is provided. Source data are provided as a Source Data file. **e** TCR repertoire analysis of OP30-reactive $V\beta7.1^+$ CTLs. Next-generation sequencing (NGS) was applied for the analysis. Source data are provided as a Source Data file. **f** Flow cytometry analysis for OP30-reactivity of PB-CTLs with TCR-expressing vector transduction. The lentivirus vectors shown in Supplementary Fig. 2f were used for the transduction. The 4-1BB expression was evaluated 24 h after OP30 exposure. The anti-CD3 antibody was used as positive control. Representative data from five independent experiments are shown. All data were gated on $CD8^+CD45^+$ live cells.

the expression of *IFNG*, *GZMB*, or *PRF1* (Supplementary Fig. 8a–c). In assays for detecting complement-dependent cytotoxicity (CDC), in which patient iPSC-derived pituitary cells were cultured with autologous serum, the number of PIT-1-positive dead cells was not increased (Supplementary Fig. 8d).

Confirmation of HLA restriction for PIT-1-reactive CTL activation and seeking a potential therapeutic strategy

Owing to in silico prediction focusing on HLA-A24 (Supplementary Fig. 1c), we isolated OP30-reactive CTLs from Case 1. Therefore, we suspected that HLA-A24 restricts the toxicity of $V\beta7.1^+$ CTLs against PIT-1-expressing cells. To confirm the HLA restriction, we used HLA-A24-overexpressing K562 cells (Supplementary Fig. 9a). We found that although individual use of either OP30- or HLA-A24-expressing K562 cells activated $V\beta7.1^+$ CTLs to some extent, robust activation was only observed when all of them were simultaneously present (Fig. 4a). Similar to the original $V\beta7.1^+$ CTLs, the pair (TRAV16/TRBV4-1) of TCR-transduced PB-CTLs were also robustly activated by OP30 under HLA-A24 restriction (Fig. 4b), whereas bulk PB-CTLs and the other pair (TRAV8-1/TRBV4-1) of TCR-transduced PB-CTLs did not show efficient activation (Supplementary Fig. 9b, c). In addition, experiments with an HLA-A24 tetramer also supported the HLA-A24 restriction for the reactive CTLs from Case 1. The CTLs efficiently bound to the OP30-loaded HLA-A24 tetramer (Fig. 4c). We utilized K562 cells overexpressing either HLA-A2 or HLA-A11 to identify which HLA molecule restricts $V\beta8^+$ CTLs from Case 2 (Supplementary Fig. 10a). OP21 robustly activated $V\beta8^+$ CTLs solely under coculture with HLA-A2 expressing K562 cells (Supplementary Fig. 10b), indicating HLA-A2 restriction for $V\beta8^+$ CTLs.

To confirm the HLA restriction, we analyzed the effect of HLA-class I blockage on reactive T cells. Under coculturing with HLA-A24-expressing K562 cells and OP30, HLA-class I antibodies suppressed the activation of reactive CTLs in a concentration-dependent manner (Fig. 4d, e). HLA-class I antibodies were also tested under different stimuli conditions. Stimuli manipulation through changing the availability of HLA-A24-expressing K562 cells (Supplementary Fig. 11a) and OP30 concentration (Supplementary Fig. 11b) revealed that the inhibitory effect of HLA-class I antibodies depended on the concentration of the stimuli. These results further supported the HLA restriction on PIT-1 reactive CTLs.

We further examined the effects of agents that potentially inhibit disease progression, specifically dexamethasone (DEX) and cyclosporin A (CsA). DEX partially inhibited PIT-1-reactive CTLs in the presence of HLA-A24 expressing K562 cells and OP30, whereas CsA notably inhibited CTL activation (Fig. 5a). Regarding CTL infiltration around PIT-1-positive cells, DEX and CsA significantly decreased the number of infiltrating cells (Fig. 5b, c). In addition, both drugs protected PIT-1-positive cells from apoptosis. Based on these results, DEX and CsA are potentially useful for treating patients with anti-PIT-1 hypophysitis.

Discussion

Many disease models employing iPSC technology have been reported, especially for genetic disorders[22]. This stems from the significant advantage of iPSCs, which enable us to generate cells and tissues of interest while maintaining the specific genetic backgrounds of patients. Indeed, HLA haplotypes, which define the specificity of the T cell immune response, can be reproduced in patient-derived iPSCs. However, modeling T cell-mediated autoimmune diseases remains challenging. Although some autoimmune disease models have been reported, they remain incomplete because the responsible T cells have not been isolated[12,23,24]. In this study, we established a disease model for anti-PIT-1 hypophysitis using iPSC technology and demonstrated the methods of isolating specific CTLs, epitopes, and corresponding HLA molecules. We also explored its potential application in drug discovery.

Previous research indicated that CTLs may play a pivotal role in the development of anti-PIT-1 hypophysitis instead of autoantibodies[15,25]. The results from ADCC and CDC assays supported that autoantibodies were not critical in disease development. More importantly, our disease model directly demonstrated the specific toxicity of CTLs against PIT-1-positive pituitary cells. Additionally, we recently reported two cases of immune checkpoint inhibitor (ICI)-related anti-PIT-1 hypophysitis, which were characterized by the presence of autoantibodies and PIT-1-reactive CTLs, and ectopic expression of PIT-1 in accompanying tumors[26]. Given that ICI treatment enhances T cell activity including self-reactive CTLs, the classification of anti-PIT-1 hypophysitis as a CTL-mediated autoimmune disease is consistent.

In anti-PIT-1 hypophysitis, concomitant malignancies with ectopic PIT-1 expression are invariably present and seem indispensable for inducing PIT-1-targeting CTLs. This paraneoplastic syndrome feature clearly distinguishes anti-PIT-1 hypophysitis from general autoimmune diseases. Considering that PIT-1 epitopes are presented on HLA molecules of pituitary cells[6], induction of PIT-1-specific CTLs and breakdown of immune tolerance are critical initial steps for autoimmunity. Although the induction of PIT-1-reactive CTLs seems reasonable as a protective response to the accompanying tumors, the mechanism of immune tolerance breakdown toward PIT-1-positive cells remains unclear. ICI-related hypophysitis[13] represents an interesting parallel, as it may involve similar tolerance breakdown mechanisms. Further investigations may shed light on these mechanisms.

In general, the antigenicity of peptides is restricted by certain HLA types in cellular immunity. For example, HLA-DQ4 or HLA-DR8 along with HLA-A2 is commonly observed in patients with type 1 diabetes mellitus[27,28]. We demonstrated that HLA-A24 was essential for the robust activation of specific CTLs by OP30 in Case 1. Given that HLA-A24 is not always shared among patients (Supplementary Table 1), other CTL-epitope-HLA combinations may be involved in disease development. We also recapitulated anti-PIT-1 hypophysitis using

https://doi.org/10.1038/s41467-025-63183-x

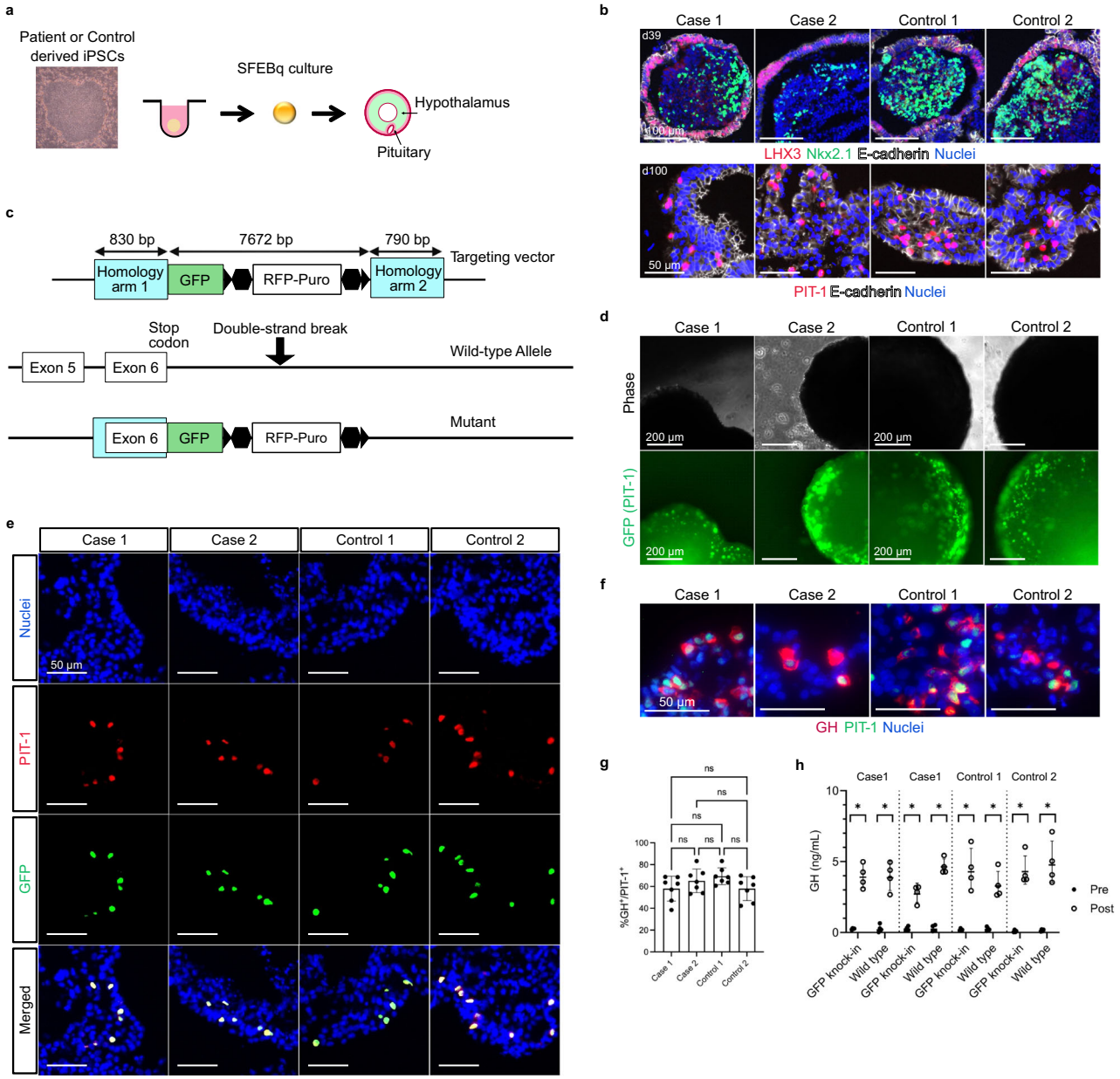

Fig. 2 | Regenerating functional PIT-1-expressing pituitary cells from patient-derived induced pluripotent stem cells (iPSCs). a Schematic presentation of pituitary cell differentiation from human iPSCs using SFEBq culture (serum-free floating culture of embryoid body-like aggregates with quick reaggregation). The outer layer cells differentiate into pituitary cells. **b** Immunofluorescence of LHX3 (pituitary progenitor cell marker), Nkx2.1 (hypothalamic cell marker), and E-cadherin (pituitary progenitor cell marker) at day 39 (upper panels) and PIT-1 and E-cadherin at day 100 (lower panels) for iPSC-derived pituitary cells. **c** The schematic of GFP knock-in targeting the human *PIT-1* locus. The *GFP* cassettes were inserted directly under the stop codon of the *PIT-1* locus. The *RFP* and *Puro* cassettes were sandwiched between loxP (arrowheads) and insulator sequences (hexagons). **d** Phase contrast and GFP images of differentiated pituitary cells at day 100. GFP^+ cells localize to the outer layer of cell organoids, in which pituitary progenitor cells reside. Scale bars: 200 μm. **e** Immunofluorescence of hoechst, PIT-1, and GFP. Scale bars: 50 μm. **f** Immunofluorescence of hoechst, PIT-1, and GH. Scale bars: 50 μm. **g** The proportion of GH^+ cells in $PIT\text{-}1^+$ cells was calculated in immunofluorescent images in (**f**). Ordinary one-way analysis of variance followed by Tukey's multiple comparisons test was used for statistical analysis. Data are presented as the mean ± standard deviation (SD). Each dot shows technical replicates from different experiments ($n = 7$). Source data are provided as a Source Data file. **h** The GH concentration in culture supernatant of each pituitary cell organoid was measured before and after 24 h of GHRH stimulation. Each dot shows technical replicates from the same pituitary organoid batches ($n = 4$). The two-sided Mann–Whitney U test was used to compare the differences in GH concentration in pre- and post-stimulated organoids. $^*P = 0.0286$. Data are presented as the mean ± SD. Representative data from two independent experiments are shown. Source data are provided as a Source Data file.

samples from Case 2 lacking HLA-A24. In the second model, $V\beta8^+$ CTLs were strongly activated in the combination of OP21 and HLA-A2, which was different from Case 1 where $V\beta7.1^+$ CTLs were activated by the combination of OP30-HLA-A24. These results confirmed the involvement of multiple combination of CTL-epitope and HLA in anti-PIT-1 hypophysitis.

This study had several limitations. Although we confirmed the reproducibility of our method, we only used samples from two patients for this disease modeling. Examination of additional cases are necessary for better understanding of the underlying pathophysiology. In addition, the establishment of the model required a relatively long time and high cost; in particular, cloning of reactive CTLs,

https://doi.org/10.1038/s41467-025-63183-x

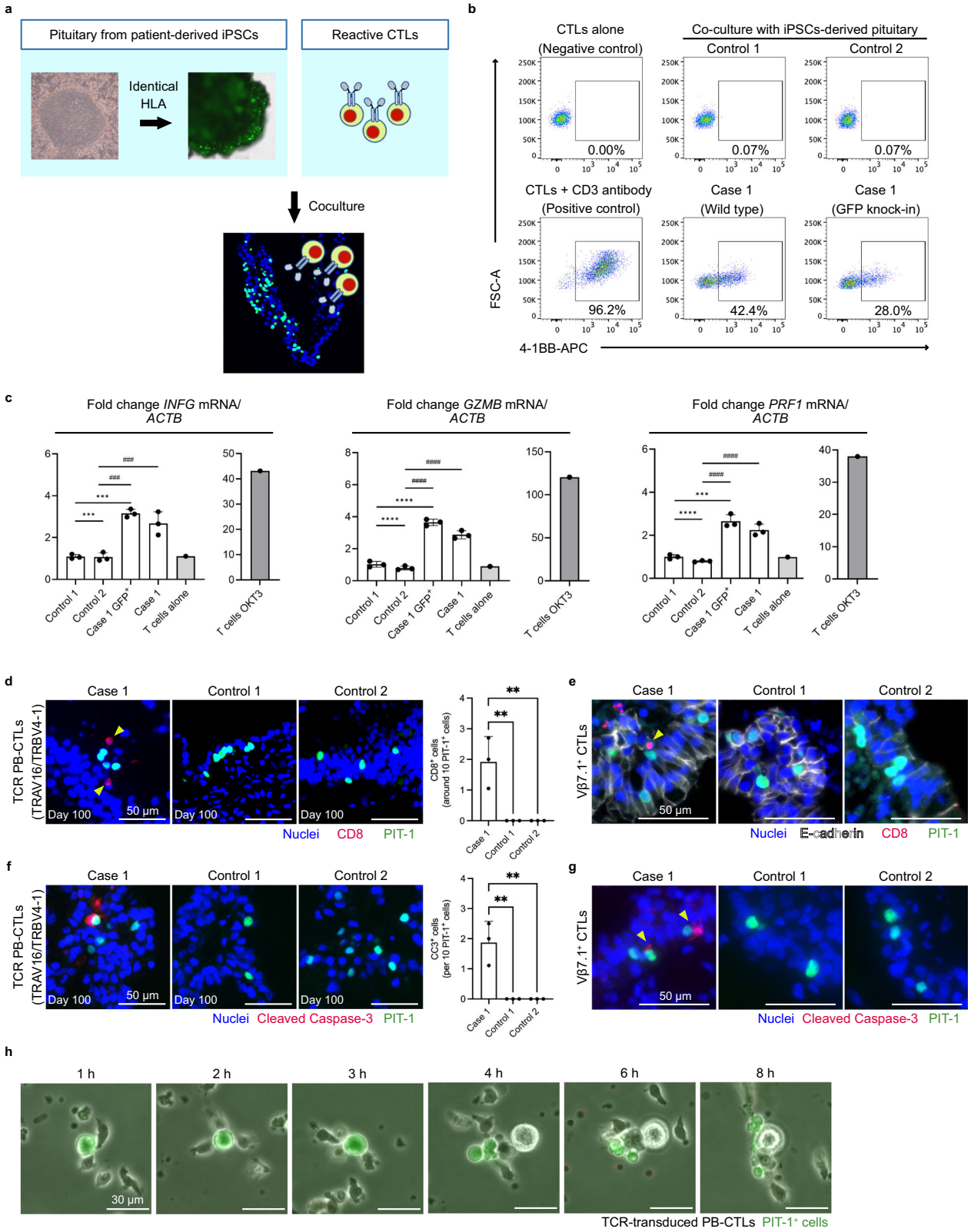

identification of responsible epitopes, and differentiation of iPSC-derived pituitary cells from clinical samples took several months. Further optimizations are needed to facilitate the application.

In conclusion, we demonstrated a novel human disease model for anti-PIT-1 hypophysitis using iPSC technology. This strategy has great potential for clarifying pathophysiology and facilitating drug discovery in various T cell-mediated autoimmune diseases.

Methods

Cell lines

Lenti-X-293T cells were purchased from Clontech (Shiga, Japan) and cultured in Dulbecco's Modified Eagle Medium (DMEM) (16971-55, Nacalai Tesque, Kyoto, Japan) supplemented with 10% fetal bovine serum (Corning, NY, USA), 2 mM L-glutamine (25030081, Thermo Fisher Scientific, MA, USA), 100 μ/mL penicillin (15140122, Thermo

Fig. 3 | Disease modeling in Case 1: Coculturing iPSC-derived pituitary organoids and reactive CTLs. OP30-reactive CTLs from Case 1 were cocultured with iPSC-derived pituitary organoids for 48 h (**a**–**g**). Vβ7.1$^+$ CTLs (**e**, **g**) and TCR-transduced CTLs with the TRAV16/TRBV4-1 pair (**b**–**d**, **f**) were used as OP30-reactive CTLs. **a** Schematic overview of coculture experiments. **b** Flow cytometry analysis regarding the reactivity of CTLs against iPSC-derived pituitary cells. The 4-1BB expression on CTLs was evaluated 48 h after coculture. The anti-CD3 antibody was used as positive control. Representative data of two independent experiments are shown. All data were gated on Kusabira-Orange$^+$ live cells. **c** qRT-PCR analysis of the expression of *GZMB*, *IFNG*, and *PRF1* ($n = 3$). Total RNA was extracted from cells after coculturing. *ACTB* was used as an internal control. Ordinary one-way analysis of variance (ANOVA) followed by Dunnett's multiple comparison tests was used for statistical analysis. $^{***}P = 0.0001$ (Case 1), and $^{***}P = 0.0007$ (Case 1 GFP$^+$), compared with Control 1; $^{\#\#\#}P = 0.0001$ (Case 1), $^{\#\#\#}P = 0.0007$ (Case 1 GFP), compared with Control 2 (*IFNG*). $^{***}P = 0.0001$ (Case 1), and $^{***}P = 0.0007$ (Case 1 GFP$^+$), compared with Control 1; $^{\#\#\#}P = 0.0001$ (Case 1), $^{\#\#\#}P = 0.0007$ (Case 1 GFP), compared with Control 2 (*IFNG*). $^{****}P = 0.0001>$, compared with Control 1; $^{\#\#\#\#}P = 0.0001>$, compared with Control 2 (*GZMB*). $^{***}P = 0.0003$ (Case 1), and $^{****}P = 0.0001>$ (Case 1 GFP$^+$), compared with Control 1; $^{\#\#\#\#}P = 0.0001>$, compared with Control 2 (*PRF1*). Data are presented as the mean ± SD. Representative data from three independent experiments are shown. Source data are provided as a Source Data file. **d**–**g** Immunofluorescence images of pituitary organoids after 48 h of coculture. Double staining of CD8 and PIT-1 (**d**, **e**) and cleaved caspase-3 (CC3) and PIT-1 (**f**, **g**) are shown. E-cadherin was also stained in (**e**). The number of CD8-positive cells within 30 μm from PIT-1-positive (**d**) and CC3-positive (**f**) cells were quantified. Each dot shows technical replicates from the identical coculture experiments ($n = 3$). Ordinary one-way ANOVA followed by Dunnett's multiple comparisons test was used for statistical analysis. Scale bars: 50 μm. $^{**}P = 0.0048$ (**d**) and $^{**}P = 0.0024$ (**f**). Data are presented as the mean ± SD. Representative data from two independent experiments are shown. Source data are provided as a Source Data file (**d**, **f**). **h** Time-lapse imaging of a coculture experiment. The GFP signal from the FITC channel was overlaid on bright field images. Nonstained cells are TCR-transduced CTLs using the TRAV16/TRBV4-1 pair. PIT-1$^+$ cells were distinguished through GFP expression. Scale bars: 30 μm. The images from a single experiment are shown.

Fisher Scientific), and 100 ng/mL streptomycin (15140122, Thermo Fisher Scientific). Wild-type K562 cells were purchased from the JCRB Cell Bank (Tokyo, Japan); HLA-A24-transduced K562 cells were provided by Dr. Masaki Yasukawa (Ehime University, Ehime, Japan)[29]. Jurkat cells were purchased from the American Type Culture Collection (ATCC; VA, USA). K562 and Jurkat cells were maintained in RPMI-1640 (49140-15, Thermo Fisher Scientific) supplemented with 10% fetal bovine serum, 2 mM L-glutamine, 100 μ/mL penicillin, and 100 ng/mL streptomycin. All cell lines were cultured at 37 °C under conditions of 21% O_2 and 5% CO_2. The mycoplasma-negative status of cells was routinely checked.

Isolation of PBMCs

Blood was obtained from patients for PBMC collection. PBMCs were isolated using the Ficoll gradient reagent (F5415, Sigma-Aldrich, MO, USA) and frozen in 10% dimethyl TC protector (KBTCP001, KAC, Hyogo, Japan).

iPSC culture

Human induced pluripotent stem cells (hiPSCs; 201B7, 409B2[17,18]), HC06[19], and AP01[6]) were obtained from RIKEN (Kobe, Japan). hiPSCs were maintained on mitomycin C-treated SNL feeder cells (ECACC, UK) in DMEM/F12 (D6421, Sigma-Aldrich) supplemented with 20% (v/v) knockout serum replacement (KSR, lot No. 1848845, Invitrogen, Lafayette, CO, USA), 0.1 mM nonessential amino acids (M7154, Sigma-Aldrich), 2 mM L-glutamine, 5 ng/mL recombinant human basic FGF (064-04543, Wako, Tokyo, Japan), and 0.1 mM 2-mercaptoethanol (135-07522, FUJIFILM, Osaka, Japan) under an atmosphere of 2% CO_2.

Establishment of iPSCs from Case 2

Briefly, 1×10^5 PBMCs isolated from Case 2 were cultured in a 24-well plate in PBMC-complete medium (StemProTM-34 SFM (10639011, Gibco, NY, USA) supplemented with 2 mM L-glutamine, 100 ng/mL SCF (193-15513, Wako), 100 ng/mL FLT-3 (067-05393, Wako), 20 ng/mL IL-6 (NIB47066000, Oriental Bio, Tokyo, Japan), and 20 ng/mL IL-3 (200-03, Peprotech, NJ, USA)) for 4 days, with half of the medium replaced daily with fresh medium. Then, cells were reprogrammed via infection with Sendai virus expressing OCT4, SOX2, KLF4, and c-MYC at a multiplicity of infection (MOI) of 10, using the CytoTune 2.0 Sendai virus kit (A16518, Thermo Fisher Scientific). Cells were cultured in PBMC-complete medium for another 6 days, then transferred to mouse embryonic fibroblast (MEF) feeders and maintained in hiPSC medium at 37 °C in a humidified atmosphere with 5% CO_2. By day 19, cells that formed reprogrammed cell clumps were manually picked up and plated on MEF-seeded 6-well plates. iPSC colonies were expanded manually for four to five passages.

Selection of iPSC clones

Regarding Case 1 (AP01 iPSC line), Control 1 (201B7 iPSC line), and Control 2 (HC06 iPSC line), one clone of each was used as wild type in the pituitary differentiation experiment. After gene-editing, 12 clones for Case 1, five clones for Control 1, and three clones for Control 2 were isolated, and one clone each was selected for pituitary differentiation based on proliferative potential, iPSC morphology, and efficiency in pituitary progenitor differentiation. For Case 2, six clones were initially chosen as wild type and narrowed down to one clone based on the same evaluation criteria described above. After gene editing, eight clones were isolated, and one clone was selected for mature pituitary differentiation based on proliferation, iPSC morphology, and efficiency in pituitary progenitor induction.

Culture of iPSC-derived pituitary cells

After removal of feeder cells using CTK solution (0.25% trypsin (25200056, Invitrogen), 0.1 mg/mL collagenase type IV (17104019, Invitrogen), 10 mM CaCl2 (06731-05, Nacalai Tesque, Kyoto, Japan), and 20% KSR in D-PBS (14249-24, Nacalai Tesque)), iPSCs were dissociated into single cells using Accutase (12679-54, Nacalai Tesque). Thereafter, 1×10^4 of the dissociated cells were plated in each well of a V-bottom low-attachment 96-well plate (Sumitomo Bakelite, Tokyo, Japan) in growth factor-free, chemically defined medium (gfCDM)[30] supplemented with 10% (v/v) KSR and 10 mM Rho-associated kinase (ROCK) inhibitor (034-24024, Wako). From day 6, 5 nM BMP-4 (314-BP, R&D Systems, Minneapolis, MN, USA) and 2 μM smoothened agonist (SAG (11914, Cayman Chemical, Ann Arbor, MI, USA)) were added. From day 18, BMP-4 was withdrawn, and organoids were maintained under high O_2 conditions (40%). From day 30, the organoids were cultured in gfCDM supplemented with 20% (v/v) KSR, and from day 60, 40 ng/ml dexamethasone (D4902, Sigma-Aldrich) was added. These organoids developed into LHX3-positive pituitary progenitor cells and subsequently differentiated into pituitary hormone-producing cells after 80 days of culture.

Immunofluorescence staining

Pituitary organoids were fixed overnight in 4% paraformaldehyde (PFA (30525-89-4, Wako) at 4 °C. The frozen sections were subjected to sucrose gradient treatment overnight prior to being embedded in Tissue-Tek O.C.T. compound (4583, Sakura Finetek, Tokyo, Japan). Cryosections (8-mm-thick) were generated using a cryostat (CM1950, Leica, Tokyo, Japan). Immunofluorescence analysis was carried out

https://doi.org/10.1038/s41467-025-63183-x

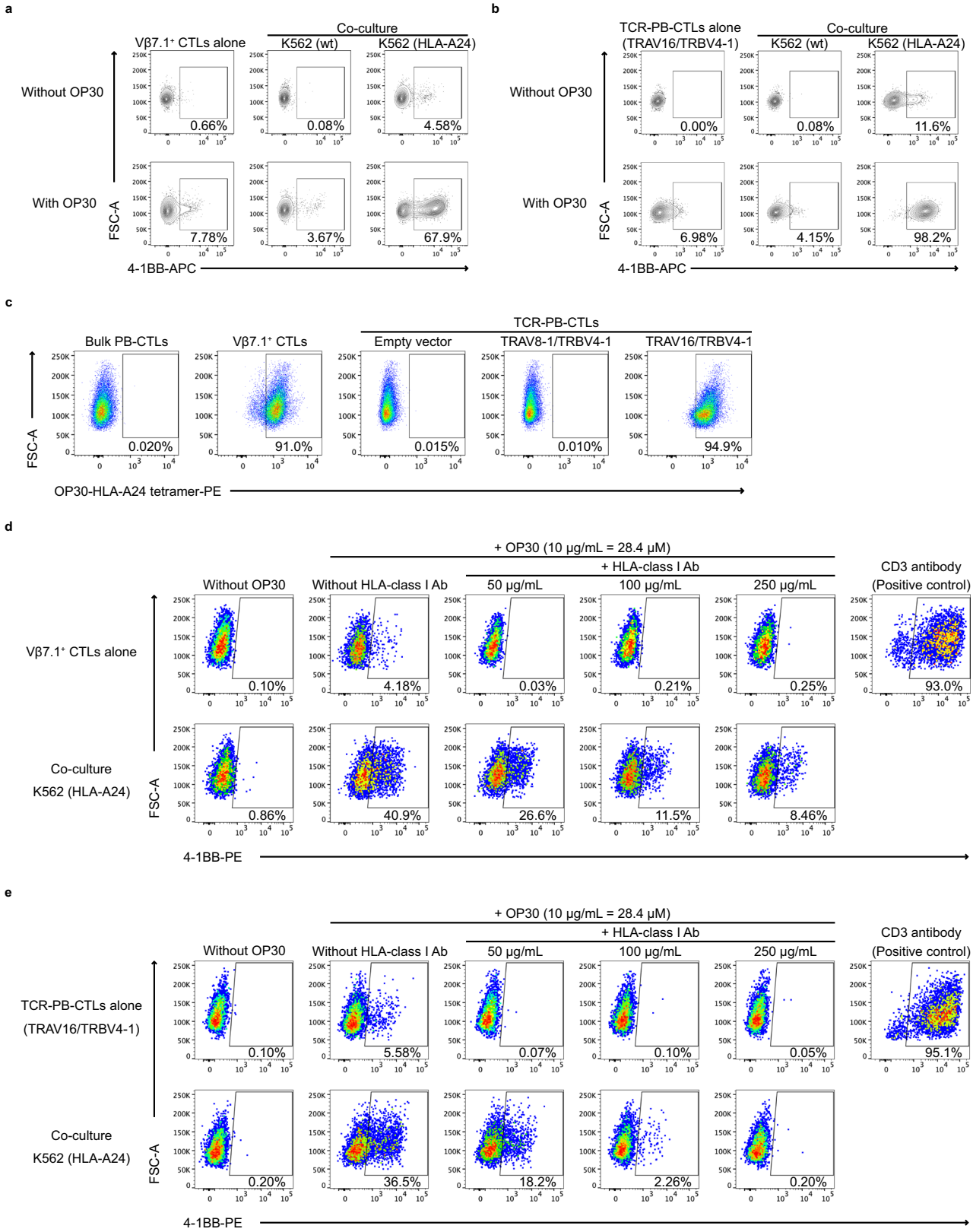

using the primary antibodies listed in Supplementary Table 3 overnight at 4 °C. Secondary antibodies used for immunofluorescent signal detection (1:1000) were goat anti-rabbit IgG Alexa Fluor 488, donkey anti-rabbit Alexa Fluor 546, goat anti-mouse Alexa Fluor 488, donkey anti-mouse Alexa Fluor 546, donkey anti-rat Alexa Fluor 647, and goat anti-rat Alexa Fluor 546 for 2 h at room temperature. Fluorescent images were obtained under a BZ-X700 microscope (Keyence, Osaka, Japan). The antibodies used in this study are summarized in Supplementary Table 3.

GH secretion assay

Twelve pituitary organoids were collected on day 100, rinsed with gfCDM, and incubated in 1 mL gfCDM at 37 °C for 10 min. For the assay, 500 μL of supernatant was collected before stimulation, followed by

Fig. 4 | HLA-A24 restriction for OP30-reactive CTLs from Case 1. a, **b** Flow cytometry analysis regarding the reactivity of CTLs against OP30 in an HLA-A24-restricted manner. The 4-1BB expression on OP30-reactive CTLs was evaluated 24 h after coculture with K562 cells. **a** Data from Vβ7.1$^+$ CTLs. Representative data from four independent experiments are shown. All data were gated on CD3$^+$CD45$^+$ live cells. **b** Data from TCR-transduced CTLs using the TRAV16/TRBV4-1 pair. Representative data from three independent experiments are shown. All data were gated on CD45$^+$ live cells. **c** Flow cytometry analysis with OP30-loaded HLA-A24 tetramer. Representative data from two independent experiments are shown for bulk PB-CTLs and Vβ7.1$^+$ CTLs. Data from a single experiment are shown for TCR-PB-CTLs. All data were gated on CD4$^-$CD8$^+$ live cells. Flow cytometry analysis regarding the effect of HLA-class I blocking on the activation of Vβ7.1$^+$ CTLs (**d**) and TCR-transduced PB-CTLs (TRAV16/TRBV4-1) (**e**). OP30 and HLA-A24 expressing K562 cells were utilized for CTL activation. CTLs were cultured for 24 h in the presence of different concentrations of HLA-class I antibody. The 4-1BB expression on CTLs was evaluated. All data were gated on CD3$^+$CD8$^+$ live cells. Representative data from three independent experiments for Vβ7.1$^+$ CTLs, and data from a single experiment for TCR-transduced PB-CTLs (TRAV16/TRBV4-1) are shown.

the addition of 500 μL gfCDM. Then, 1 μg/mL human GHRH (334-41271, FUJIFILM) was added and incubated at 37 °C for 24 h. Pre- and post-stimulated samples were subjected to ELISA using the Elecsys human GH kit (05390125190, Roche Diagnostics, Zug, Switzerland).

Enzyme-linked immunospot assay (ELISpot)

ELISpot assays were performed using ELISpotPro for human IFN-γ (3420-2APT-2, Mabtech, Stockholm, Sweden), following the manufacturer's instructions. Briefly, 2.5×10^5 isolated PBMCs were seeded in each well and incubated with OPs (10 μg/mL) in 96-well microtiter plates precoated with 10 μg/mL anti-human IFN-γ antibody for 40 h. After washing, 1 μg/mL of anti-human IFN-γ detection antibody was added, and the cells were incubated for 2 h. The cells were then incubated with streptavidin-alkaline phosphatase for 1 h, followed by development with 0.45-μm filtered 5-bromo-4-chloro-3-indolyl-phosphate/nitro blue tetrazolium substrate solution for 10–20 min. Stimulation with anti-CD3 antibody was used as the positive control. The spots were scanned on ImmunoSpot 7.0.37.0 (C.T.L, OH, USA).

Depletion of CD4$^+$CD25$^+$ cells using magnetic-activated cell sorting

The CD4$^+$ population was separated from 1×10^7 patient-derived PBMCs using a CD4$^+$ T cell isolation kit (130-096-533, Miltenyi Biotec, Bergisch Gladbach, Germany). After the first nonlabeled separation of CD4$^+$ cells, the cells were labeled with CD25-PE antibody (302605, BioLegend, CA, USA). Thereafter, the CD4$^+$CD25$^+$ population was removed using anti-PE MicroBeads UltraPure (130-105-639, Miltenyi Biotec). The remaining populations, that is, CD4$^+$-depleted cells from the first separation and CD4$^+$CD25$^+$-depleted cells from the second separation, were combined to prepare CD4$^+$CD25$^+$-depleted PBMCs.

Concentrating reactive T cell population from CD4$^+$CD25$^+$-depleted PBMCs

CD4$^+$CD25$^+$-depleted PBMCs were exposed to 10 μg/mL of each OPs every 2 weeks. After four repeated exposures, a specific T cell population was confirmed based on 4-1BB expression upon restimulation with OPs. Then, the 4-1BB$^+$ T cells gated on specific Vβ-subtype were sorted for further expansion. During the entire process, the cells were cultured in T cell medium in the presence of 100 μ/mL IL-2 (200-02, Peprotech). The T cell medium consisted of RPMI-1640, 10% pooled heat-inactivated human AB serum (12181301C, COSMO BIO, Tokyo, Japan), 2 mM L-glutamine, 100 μ/mL penicillin, and 100 ng/mL streptomycin.

T cell reactivity assays against OPs

For this assay, 1×10^5 T cells were incubated in 96-well U-bottom plates in T cell medium in the presence of 10 μg/mL OPs, 100 μ/mL IL-2, 5 ng/mL IL-7 (200-07, Peprotech), and 5 ng/ml IL-15 (200-15, Peprotech). For CD107a staining, CD107a antibody (VP008, BD Bioscience, NJ, USA) and 2 μM monensin (420701, BioLegend) were added before peptide exposure. After incubation, T cells were stained for CD107a and other markers for flow cytometry.

Phytohemagglutinin/PBMC expansion method

The expansion method was applied to expand the following T cells: bulk, empty vector-transduced, TCR-transduced, Vβ7.1$^+$ and Vβ8$^+$ PB-CTLs. The T cells were cocultured with irradiated (40 Gy) allogeneic PBMCs, which served as feeder cells, at a ratio of 1:10. T cell medium was supplemented with 5 ng/mL IL-7, 5 ng/mL IL-15, and 2 μg/mL phytohemagglutinin (161-15251, Wako, Osaka, Japan). Half of the medium without phytohemagglutinin was replaced every other day.

NGS-based TCR repertoire analysis

OP30-reactive Vβ7.1$^+$ CTLs (Supplementary Fig. 2b–e) were collected and submitted to Repertoire Genesis Incorporation. The results are shown in Fig. 1e. NGS-based TCR repertoire analysis was performed by Repertoire Genesis Inc. (Osaka, Japan).

Total RNA was extracted from PBMCs using the RNeasy Lipid Tissue Mini Kit (74804, Qiagen, Limburg, Germany) following the manufacturer's instructions. RNA concentration and purity were measured using the Agilent 2200 TapeStation (Agilent Technologies, CA, USA). Next-generation sequencing (NGS) was performed using unbiased TCR repertoire analysis technology (Repertoire Genesis Inc.)[31,32], with some modifications. All primer sequences used in repertoire analysis are listed in Supplementary Table 4. Total RNA was converted to complementary DNA (cDNA) using the Superscript III reverse transcriptase (18-080-085, Invitrogen). The BSL-18E primer containing polyT_{18} and a NotI site was used for cDNA synthesis. After cDNA synthesis, double strand (ds)-cDNA was synthesized using E. coli DNA polymerase I (18010017, Invitrogen), E. coli DNA ligase (18052019, Invitrogen), and RNase H (18021014, Invitrogen). Double-strand cDNAs were blunted using T4 DNA polymerase (18005025, Invitrogen). The P10EA/P20EA adaptor was ligated to the 5′ end of the ds-cDNA and then cut with NotI restriction enzyme (1166A, Takara Bio, Shiga, Japan). After removal of the adaptor and primer using the MinElute Reaction Cleanup kit (28204, Qiagen), PCR was performed using the KAPA HiFi DNA polymerase (07958846001, Roche Diagnostics) with the first PCR primer pair (primer specific to the constant region of each gene/P20EA). PCR conditions were as follows: 98 °C (20 s), 60 °C (30 s), and 72 °C (1 min) for 20 cycles. The second PCR was performed using the second PCR primer pair (gene-specific second PCR primer/P20EA) using the same PCR conditions. Amplicons were prepared by amplification of the second PCR products using the Tag primer pair (gene-specific Tag PCR primer/P22EA-ST1-R). PCR conditions were as follows: 98 °C (20 s), 60 °C (30 s), and 72 °C (1 min) for 20 cycles. After PCR amplification, index (barcode) sequences were added by amplification using the Nextera XT index kit v2 setA or setD (FC-131-2001, Illumina, CA, USA). The indexed amplicon products were mixed in an equal molar concentration and quantified using a Qubit 2.0 Fluorometer (MAN0003231, Thermo Fisher Scientific). Sequencing was conducted using the Illumina Miseq paired-end platform (2 × 300 bp).

All paired-end reads were classified by index sequences. Sequences assignment was performed by determining sequences with the highest identity in a data set of reference sequences from the international ImMunoGeneTics information system (IMGT) database (http://www.imgt.org). Data processing, assignment, and data

https://doi.org/10.1038/s41467-025-63183-x

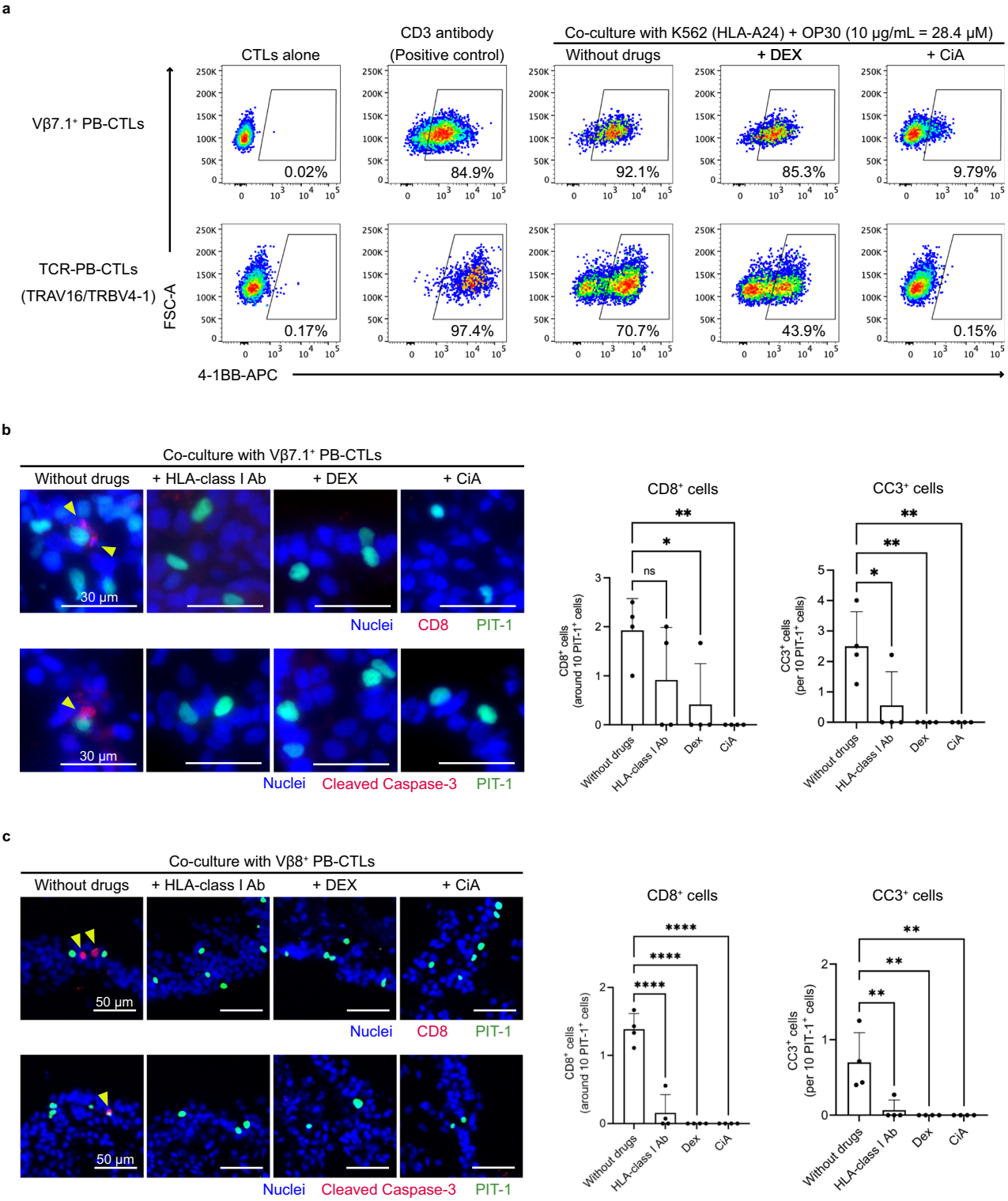

Fig. 5 | Treatment screening model for anti-PIT-1 hypophysitis. a Flow cytometry analysis regarding the inhibitory effects of drugs on CTL activation. CTLs were cocultured with K562 cells in the presence of high-dose OP30 (10 μg/mL = 28.4 μM). Data were acquired 24 h after coculture. All data were gated on $CD3^+CD45^+$ live cells. Representative data from four independent experiments for $Vβ7.1^+$ CTLs, and from two independent experiments for TCR-transduced CTLs using the TRAV16/TRBV4-1 pair are shown. The effect of drugs on the migration and cytotoxicity of $Vβ7.1^+$ CTLs from Case 1 (**b**) and $Vβ8^+$ CTLs from Case 2 (**c**). Immunofluorescence images of pituitary organoids after 48 h of autologous coculture are shown ($n = 4$). Double staining of CD8 and PIT-1 is shown on the upper row and cleaved caspase-3 (CC3) and PIT-1 on the lower row. CD8-positive cells within 30 μm from PIT-1-positive and CC3-positive cells were counted. Scale bars for (**b**) and (**c**) are 30 μm and 50 μm, respectively. Each dot shows technical replicates from the identical coculture experiments ($n = 4$). Ordinary one-way analysis of variance followed by Dunnett's multiple comparisons test was used for statistical analysis. $^{****}P = 0.0001$ > for $CD8^+$ cells, and $^*P = 0.0126$ and $^{**}P = 0.022$ for $CC3^+$ cells in (**b**). $^{**}P = 0.0028$ (Without drugs vs. HLA-class I Ab) and $^{**}P = 0.0013$ (Without drugs vs. Dex, and Without drugs vs. CiA) for $CD8^+$ cells, and $^*P = 0.0126$ and $^{**}P = 0.022$ for $CC3^+$ cells in (**c**). Data are presented as the mean ± SD. Representative data from three independent experiments for (**b**) and two independent experiments for (**c**) are shown. Source data are provided as a Source Data file (**b**, **c**).

aggregation were automatically performed using the repertoire analysis software Repertoire Genesis (RG) originally developed by Repertoire Genesis Inc. RG implemented a program for sequence homology searches using BLATN, an automatic aggregation program, a graphics program for gene usage, and CDR3 length distribution. Sequence identities at the nucleotide level between query and entry sequences were automatically calculated. Parameters that increased sensitivity and accuracy (E-value threshold, minimum kernel, and high-scoring segment pair (HSP) score) were carefully optimized for respective repertoire analysis. Nucleotide sequences of CDR3 regions spanning from the conserved cysteine at position 104 (Cys104) to the conserved phenylalanine or tryptophan at position 118 (Phe118 or Trp118) according to IMGT nomenclature were translated into deduced amino acid sequences. A unique sequence read (USR) was defined as a sequence read that shared no identical gene segment assignment or deduced CDR3 amino acid sequence with any other sequence read. The copy number of identical USR was automatically counted in each sample and ranked using the RG software. The frequencies of V, D, J, and C gene-containing sequence reads were calculated as percentages of total reads.

Preparation of OP30-HLA-A24 tetramer

OP30 peptides were loaded onto the QuickSwitch Quant HLA-A∗24:02 tetramers (PE labeled) (TS-7302-1R, MBL International, Tokyo, Japan) according to the manufacturer's protocol.

Preparation and transduction of TCR-expressing lentiviral vectors

cDNA was synthesized from mRNA extracted from OP30-reactive Vβ7.1$^+$ PB-CTLs. Using the primers listed in Supplementary Table 4, full-length TCRA and TCRB were selectively amplified. After obtaining the TCRB-P2A-TCRA sequence through ligation, the sequence was inserted into the lentiviral vector, CS-UbC-RfA-IRES2-hKO1, controlled by the human ubiquitin C (UbC) promoter. Lentiviral vector production was performed using Lenti-X-293T cells (632180, Clontech, CA, USA) according to the manufacturer's protocol. After 2 days of stimulation with plate-bound CD3 Ab (317315, Thermo Fisher Scientific) and 1 μg/mL soluble CD28 Ab (302934, Thermo Fisher Scientific), bulk PB-CTLs were exposed to the lentivirus at a multiplicity of infection (MOI) of 20. The culture medium was completely changed after 24 h of lentiviral exposure. The KO$^+$ population was sorted using flow cytometry to concentrate TCR-transduced PB-CTLs.

Preparation and transduction of TCR-expressing retroviral vectors

Amplified genes for full-length TCRA and TCRB were inserted into the pMY retroviral vector (RTV-020, Cell BioLabs, San Diego, CA, USA) using the In-fusion HD Cloning Kit (102518, Takara Bio). The primers used are listed in Supplementary Table 4. Retroviral vector production was performed using GP2-293 cells (631458, Takara Bio) according to the manufacturer's protocol. After 2 days of stimulation with plate-bound CD3 Ab and 1 μg/mL soluble CD28 Ab, bulk PB-CTLs were exposed to the retroviruses at a MOI of 10. The Tag-BFP$^+$ population was sorted using flow cytometry to concentrate TCR-transduced PB-CTLs.

Generation of HLA-A2 or HLA-A11 expressing K562 cells

Full-length cDNA for HLA-A*02:01:01 or HLA-A*11:01:01 was purchased from RIKEN BRC (Ibaraki, Japan). The sequence was then ligated between the BamHI and XhoI sites of the pMY retroviral vector, digested with BamHI (R0136T, NEB, MA, USA) and XhoI (R0146L, NEB). To generate genetically engineered K562 cells expressing HLA-A2 or HLA-A11, K562 cells were seeded into 6-well plates at 3×10^5 cells/well and then transduced with the retrovirus at a MOI of 10. Two weeks after transduction, Tag-BFP-positive cells were sorted.

Generation of PIT-1-GFP reporter iPSCs using CRISPR/Cas9 and targeting vector

Using homologous recombination with CRISPR/Cas9, we designed a fusion protein of PIT-1 and GFP for expression by inserting the PIT-1 locus into the HR120PA-1 vector (HR120PA-1, System Biosciences, CA, USA). For the sgRNA/Cas9 expression vector, the 5′-CACCTTTTCT CCCGTTTCATTCCT-3′ and 5′-AAACAGGAATGAAACGGGAGAAAA-3′ sequences were cloned into the sgRNA scaffold of pSpCas9(BB)-2A-Puro (pX459) (62988, Addgene, MA, USA). Briefly, 1 μg of plasmid was digested with BbsI (ER1012, Thermo Fisher Scientific) for 30 min at 37 °C, and the two oligos were annealed with 10× T4 ligation buffer (B0202S, NEB) and T4PNK (M0236L, NEB) using the following parameters: 37 °C for 30 min, 95 °C for 5 min, and cooling to 25 °C at 5 °C/min. These oligos were cloned into the digested plasmid using Quick Ligase (M2200L, NEB). For creating the targeting vector, 5′ and 3′ homology arms (0.83 kb and 0.79 kb, respectively) of PIT-1 were amplified from the genomic DNA of iPSCs using the following primers: 5′-GCCGAATTCCTAAGAGACTGGCCATATCTTCTC-3′ and 5′CGGGATC CATGTCTTGTTATAGAAACCTGGATG-3′ for the 5′ homology arm, and 5′-CGGGATCCCAAAAACAGAAATTACTTGGTTGAC-3′ and 5′CGCGAAT TCTCTGCACTCAAGATGTTCCTTAG-3′ for the 3′ homology arm. The 5′ homology arm was cloned into the EcoRI site of the HR120PA-1 vector, and the 3′ homology arm was cloned into the BamHI site using an In-fusion HD Cloning Kit.

The sgRNA/Cas9 expression and targeting vectors were transfected into human iPSCs using the Lipofectamine Stem Transfection Reagent (STEM00001, Thermo Fisher Scientific). Puromycin-resistant strains were obtained, and the genome sequence was confirmed by direct sequencing using the following primers: 5′- GGAGAACAGAA-TAAACCTTCTTCT-3′, 5′-GGGCAGGCCGCTCTCGTC-3′, 5′-GGTTTGTCC AAACTCATCAATG-3′, and 5′-GGTTTGTCCAAACTCATCAATG-3′.

ADCC and CDC assays

GFP$^+$ pituitary organoids were prepared from Case 1. PBMCs and serum samples were prepared from Case 1 and healthy donors, Controls 1 and 2. Serum samples were stored at −80 °C without the addition of preservatives. The sera were diluted in gfCDM. All samples were prepared in triplicate. Assay cultures were performed for 24 h at 37 °C in 96-well U-bottom plates. At the end of the culture, pituitary organoids were collected and washed twice with D-PBS. Then, they were dissociated into single cells by treating with Accumax (17087-54, Nacalai Tesque) for 25 min at 37 °C. The cells were filtered using a 100-μm cell strainer and stained for flow cytometry analysis with CD45-Pacific Blue antibody (368539, BioLegend) and Fixable Viability Dye eFluor 780 (eFluor-780) (65-0865-14, eBioscience, CA, USA) in 2% FBS on ice for 25 min. For the experimental positive control, pituitary organoids were treated with tunicamycin (11445, Cayman Chemical) under the indicated concentrations. Percentage cytotoxicity was calculated as follows:

$$\begin{aligned} &Percentage\ living PIT-1^+ cells \\ &= (eFluor-780^- PIT-1^+ cells / PIT-1^+ cells) \times 100 \end{aligned} \quad (1)$$

In the ADCC assay, PBMCs from either Case 1 or healthy donors were used as effector cells. The serum origin was matched to the individuals of effector cells. Two pieces of the GFP$^+$ pituitary organoids were applied to each well with 100 μL of gfCDM. Subsequently, 50 μL each of 2×10^5 effector cell suspension and serum were added to the wells with the pituitary organoids for ADCC assay culture.

In the CDC assay, three pieces of the GFP$^+$ pituitary organoids were applied to each well with 100 μL of gfCDM. Subsequently, 100 μL of serum was added to the wells with the pituitary organoids for CDC assay culture.

Time-lapse imaging

The iPSC-derived pituitary tissues were dissociated using TrypLE Express Enzyme (12-604-013, Thermo Fisher Scientific). GFP$^+$ cells from the dissociated iPSC-derived pituitary tissues were detected using the FITC channel on a FACSAria flow cytometer (BD Bioscience), and sorted before time-lapse imaging. The pituitary cells were cocultured with the PIT-1-GFP reporter and TCR-transduced PB-CTLs in phenol red-free DMEM (044-32955, Wako) supplemented with 10% pooled heat-inactivated human AB serum, 2 mM L-glutamine, 100 μ/mL penicillin, 100 ng/mL streptomycin, 100 μ/mL IL-2, 5 ng/mL IL-7, and 5 ng/mL IL-15. Propidium iodide (1 μg/mL) (537060, Sigma-Aldrich) was also added for dead cell staining. Images were captured on BioStation IM-Q (Nikon, Tokyo, Japan) for 2 d. The GFP signal from the FITC channel was overlaid onto bright-field images. The captured images were edited using EDIUS Neo 3.5 (Grass Valley, Montreal, QC, Canada).

Coculture experiments (CTLs vs. pituitary)

Coculture experiments were conducted in the presence of 100 μ/mL IL-2, 5 ng/mL IL-7, and 5 ng/mL IL-15; 50 μg/mL of HLA class I blocking antibody (311428, BioLegend), 4 μg/mL dexamethasone (D4902, Sigma-Aldrich), and 10 μg/mL cyclosporin A (59865-13-3, FUJIFILM) were used for inhibitor experiments. iPSC-derived pituitary organoids with abundant GFP$^+$ cells were cocultured with 1×10^5 T cells in 96-well U-bottom plates. For coculturing, T cell and pituitary media were mixed at a ratio of 3:1. After 48 h of coculture, samples were collected for analysis.

Coculture experiments (CTLs vs. K562)

Briefly, T cells and K562 cells (1×10^5 each) were cocultured in 96-well U-bottom plates for 24 h. T cell medium was used for the coculture experiments. Under OP30-supplemented conditions, the concentration was fixed at 10 μg/mL.

Flow cytometry

Data were acquired using an LSRFortessa (BD Bioscience) or FACSAria flow cytometer (BD Bioscience) and analyzed with the FlowJo software (Tree Star, NJ, USA). The antibodies used in this study are summarized in Supplementary Table 3.

In the analysis of pituitary-derived cells, to separate cells derived from the oral ectoderm and hypothalamic tissue, pituitary organoids were subjected to flow cytometry. After washing organoids twice with PBS, they were dissociated into single cells treated with 5 mM EDTA/HBSS for 20 min. The cells were then filtered using a 70-μm cell strainer and incubated with antibodies in 2% FBS on ice for 25 min. After washing twice, the cells were resuspended in 2% FBS and analyzed. For detecting GFP$^+$ cells, the FITC channel was applied.

In the analysis of T cells, T cells were washed in PBS supplemented with 2% FBS and stained with the appropriate antibodies for 30 min at 4 °C in the dark. After staining, the cells were washed, and 1 μg/mL propidium iodide was added to exclude dead cells. The Beta Mark TCR Vβ Repertoire Kit (IM3497, Beckman Coulter, CA, USA) was used to access the TCR Vβ repertoire. For detecting Kusabira-Orange$^+$ and Tag-BFP$^+$ cells, the green PE and Pacific Blue channels were applied, respectively.

Quantitative real-time PCR

Total RNA was extracted from cells using the NucleoSpin RNA XS kit (U0902B, Takara Bio). The total RNA was subjected to reverse transcription using the ReverTra Ace qPCR RT Kit (FSQ-101, TOYOBO, Osaka, Japan). Quantitative PCR was performed using the StepOnePlus Real-Time PCR system (Applied Biosystems, MA, USA). The thermal cycling profile was as follows: initial denaturation at 95 °C for 15 min, followed by 40 cycles of denaturation at 95 °C for 15 s, annealing at 60 °C for 30 s, and extension at 72 °C for 15 s. Relative mRNA expression level was determined using the $2^{-\Delta\Delta CT}$ method, and *ACTB* or *HPRT-1* was used as the internal control. The cut-off value was <35 cycles. The primer sequences used are listed in Supplementary Table 4. All samples were assayed in triplicate.

Peptide synthesis

Peptide synthesis was performed by Scrum, Inc (Tokyo, Japan). The peptides were analyzed using mass spectrometry and high-performance liquid chromatography (HPLC). In the case of a sequence whose N-terminal was Q, a possibility existed that it had a cyclic structure, pGlu, under weakly acidic conditions; therefore, the sequence whose N-terminal was Q had a single residue of the previous amino acid added. Example: No2 QAFTSADTFI (10AA)→DQAFTSADTFI (11AA).

Epitope prediction algorithms

The following prediction algorithms were applied for predicting HLA-A24:02-restricted epitopes in PIT-1.

BMAS: (http://www-bimas.cit.nih.gov/molbio/hla_bind/).

SYFPEITHI: (http://www.syfpeithi.de/bin/MHCServer.dll/EpitopePrediction.htm).

NetMHCcons-1.1: (http://www.cbs.dtu.dk/services/NetMHCcons/).

Statistical analysis

Data are expressed as the mean ± standard deviation. One-way analysis of variance (ANOVA) followed by either Tukey's multiple comparison test or Dunnett's multiple comparisons test was used to assess significance levels in parametric analysis. Mann–Whitney U test was used in nonparametric analysis. Geisser-Greenhouse's correction was applied for repeated-measures ANOVA, and *F* approximation with estimated degrees of freedom was calculated. Significance levels were set at $^*P < 0.05$, $^{**}P < 0.01$, $^{***}P < 0.001$, $^{****}P < 0.0001$. Statistical analysis was performed using the JMP Statistical Database Software version 14.0.0 (SAS Institute, Cary, NC, USA). Graphs were generated, and statistical analyses were performed using GraphPad Prism (GraphPad Software, CA, USA).

Contact for reagent and resource sharing

Further information and requests for resources and reagents might be directed to and will be fulfilled by the Lead Contact, Yutaka Takahashi (takahash@naramed-u.ac.jp).

Study approval

The Medical Ethics Review Committee of Kobe University Graduate School of Medicine approved this study (approval number 1685). All methods were performed in accordance with the relevant guidelines, and all uses of human material have been approved by the Medical Ethics Review Committee, Clinical and Translational Research Center, Kobe University Hospital (approval number 29-62). The patients and healthy donors provided written informed consent.

Reporting summary

Further information on research design is available in the Nature Portfolio Reporting Summary linked to this article.

Data availability

No datasets were generated or analyzed during the current study. All data are included in the Supplementary Information or available from the authors, as are unique reagents used in this Article. The raw numbers for charts and graphs are available in the Source Data file whenever possible. The dataset associated with the manuscript is stored in the figshare repository (https://doi.org/10.6084/m9.figshare.24320965)[33]. Source data are provided with this paper.

References

1. Yamamoto, M. et al. Autoimmune pituitary disease: new concepts with clinical implications. *Endocr. Rev.* **41**, bnz003 (2020).
2. Takahashi, Y. Mechanisms in endocrinology: autoimmune hypopituitarism: novel mechanistic insights. *Eur. J. Endocrinol.* **182**, R59–r66 (2020).
3. Bando, H. et al. Paraneoplastic autoimmune hypophysitis: an emerging concept. *Best. Pract. Res. Clin. Endocrinol. Metab.* **36**, 101601 (2021).
4. Yamamoto, M. et al. Adult combined GH, prolactin, and TSH deficiency associated with circulating PIT-1 antibody in humans. *J. Clin. Invest.* **121**, 113–119 (2011).
5. Bando, H. et al. Involvement of PIT-1-reactive cytotoxic T lymphocytes in anti-PIT-1 antibody syndrome. *J. Clin. Endocrinol. Metab.* **99**, E1744–E1749 (2014).
6. Kanie, K. et al. Pathogenesis of anti-PIT-1 antibody syndrome: PIT-1 presentation by HLA class I on anterior pituitary cells. *J. Endocr. Soc.* **3**, 1969–1978 (2019).
7. Tzou, S. C. et al. Autoimmune hypophysitis of SJL mice: clinical insights from a new animal model. *Endocrinology* **149**, 3461–3469 (2008).
8. Lin, H. H. et al. In situ activation of pituitary-infiltrating T lymphocytes in autoimmune hypophysitis. *Sci. Rep.* **7**, 43492 (2017).
9. Watanabe, K. et al. Characteristics of experimental autoimmune hypophysitis in rats: major antigens are growth hormone, thyrotropin, and luteinizing hormone in this model. *Autoimmunity* **33**, 265–274 (2001).
10. Klein, I., Kraus, K. E., Martines, A. J. & Weber, S. Evidence for cellular mediated immunity in an animal model of autoimmune pituitary disease. *Endocr. Res. Commun.* **9**, 145–153 (1982).
11. Young, J. E. et al. Elucidating molecular phenotypes caused by the SORL1 Alzheimer's disease genetic risk factor using human induced pluripotent stem cells. *Cell. Stem Cell.* **16**, 373–385 (2015).
12. Matsumoto, R. et al. Congenital pituitary hypoplasia model demonstrates hypothalamic OTX2 regulation of pituitary progenitor cells. *J. Clin. Investig.* **130**, 641–654 (2020).
13. Leite, N. C. et al. Modeling Type 1 diabetes in vitro using human pluripotent stem cells. *Cell Rep.* **32**, 107894 (2020).
14. Pedersen, N. W. et al. CD8+ T cells from patients with narcolepsy and healthy controls recognize hypocretin neuron-specific antigens. *Nat. Commun.* **10**, 837 (2019).
15. Urai, S. et al. Clinical features of anti-pituitary-specific transcription factor-1 (PIT-1) hypophysitis: a new aspect of paraneoplastic autoimmune condition. *Eur. J. Endocrinol.* **190**, K1–k7 (2024).
16. Sugiyama, D. et al. Anti-CCR4 mAb selectively depletes effector-type FoxP3+CD4+ regulatory T cells, evoking antitumor immune responses in humans. *Proc. Natl Acad. Sci. USA* **110**, 17945–17950 (2013).
17. Takahashi, K. et al. Induction of pluripotent stem cells from adult human fibroblasts by defined factors. *Cell* **131**, 861–872 (2007).
18. Okita, K. et al. A more efficient method to generate integration-free human iPS cells. *Nat. Methods* **8**, 409–412 (2011).
19. Ishida, Y. et al. Vulnerability of Purkinje cells generated from spinocerebellar ataxia type 6 patient-derived iPSCs. *Cell Rep.* **17**, 1482–1490 (2016).
20. Ozone, C. et al. Functional anterior pituitary generated in self-organizing culture of human embryonic stem cells. *Nat. Commun.* **7**, 10351 (2016).
21. Suga, H. et al. Self-formation of functional adenohypophysis in three-dimensional culture. *Nature* **480**, 57–62 (2011).
22. Jin, M. et al. Type-I-interferon signaling drives microglial dysfunction and senescence in human iPSC models of Down syndrome and Alzheimer's disease. *Cell. Stem Cell.* **29**, 1135–1153.e8 (2022).
23. Crawford, M. P. et al. High prevalence of autoreactive, neuroantigen-specific CD8+ T cells in multiple sclerosis revealed by novel flow cytometric assay. *Blood* **103**, 4222–4231 (2004).
24. Latorre, D. et al. T cells in patients with narcolepsy target self-antigens of hypocretin neurons. *Nature* **562**, 63–68 (2018).
25. Bando, H. et al. A novel thymoma-associated autoimmune disease: Anti-PIT-1 antibody syndrome. *Sci. Rep.* **7**, 43060 (2017).
26. Urai, S. et al. Anti-PIT1 hypophysitis after immune checkpoint inhibitor treatment. *Nat. Rev. Endocrinol.* **21**, 265–266 (2025).
27. Nejentsev, S. et al. Localization of type 1 diabetes susceptibility to the MHC class I genes HLA-B and HLA-A. *Nature* **450**, 887–892 (2007).
28. Tan, S. et al. Type 1 diabetes induction in humanized mice. *Proc. Natl Acad. Sci. USA* **114**, 10954–10959 (2017).
29. Miyazaki Y. et al. Development of a novel redirected T cell–based adoptive immunotherapy targeting human telomerase reverse transcriptase for adult T cell leukemia. *Blood*. **121**, 4894–4901 (2013).
30. Wataya, T. et al. Minimization of exogenous signals in ES cell culture induces rostral hypothalamic differentiation. *Proc. Natl Acad. Sci. USA* **105**, 11796–11801 (2008).
31. Kitaura, K. et al. A new high-throughput sequencing method for determining diversity and similarity of T cell receptor (TCR) α and β repertoires and identifying potential new invariant TCR α chains. *BMC Immunol.* **17**, 38 (2016).
32. Kitaura, K. et al. Different somatic hypermutation levels among antibody subclasses disclosed by a new next-generation sequencing-based antibody repertoire analysis. *Front Immunol.* **8**, 389 (2017).
33. Kanie, K. Modeling of T cell-mediated autoimmune pituitary disease using human induced pluripotent stem cell-induced organoid. figshare https://doi.org/10.6084/m9.figshare.24320965 (2025).

Acknowledgements

This work was partially supported by the Grants-in-Aid for Scientific Research from JSPS KAKENHI 18K08514 (G.I.), 23659477 (G.I.), 21KK0149 (H.B.), 21K20933 (K.K.), 22K16396 (K.K.), and 25K19653 (K.K.), the Japan Agency for Medical Research and Development (AMED) 17bm0804012h0001 (Y.T.), Collaborative Research Grant from Japan Endocrine Society 2025 (Y.T.), and the Ministry of Health, Labor and Welfare (Hypothalamo-hypophyseal Disorders and Endocrine Syndrome with Sexual Differentiation and Maturation) (Y.T.). We thank Professor Takuya Yamamoto for providing the culture environment for the iPSC-derived pituitary cells. Supplementary Fig. 5a was created using BioRender.com (https://BioRender.com/siz05p5).

Author contributions

K.K., T.I., G.I., Shin.K., and Y.T. conceived the study and designed the experiments. K.K. and T.I. performed the experiments. R.M. advised on the study. K.M. established the patient- and donor-derived iPSCs. K.K. T.I., and Y.T. wrote the manuscript. S.U., Shuichi.K., H.B., M.Y., H.F., and W.O. contributed to the discussion. All authors have read and approved the final version of the manuscript.

Competing interests

Yutaka Takahashi has received research funding from Teijin Pharma Co., Ltd. and Ono Pharma Co., Ltd. Shin Kaneko is a founder, shareholder, and director of Thyas Co., Ltd. and has received research funding from Takeda Pharmaceutical Co., Ltd., Astellas Co., Ltd., Kirin Co., Ltd., Terumo Co., Ltd., and Thyas Co., Ltd. The other authors have nothing to declare.

Additional information

Supplementary information The online version contains supplementary material available at https://doi.org/10.1038/s41467-025-63183-x.

Correspondence and requests for materials should be addressed to Yutaka Takahashi.

Peer review information *Nature Communications* thanks George Chrousos, Teddy Fauquier and Anette Wolf for their contribution to the peer review of this work. A peer review file is available.